

# Origin of the anomalous long lifetime of $^{14}\text{C}$

P. Maris,<sup>1</sup> J.P. Vary,<sup>1</sup> P. Navrátil,<sup>2,3</sup> W. E. Ormand,<sup>3,4</sup> H. Nam,<sup>5</sup> and D. J. Dean<sup>5</sup>

<sup>1</sup>*Department of Physics and Astronomy, Iowa State University, Ames, Ia 50011-3160, USA*

<sup>2</sup>*TRIUMF, 4004 Wesbrook Mall, Vancouver BC, V6T 2A3, Canada*

<sup>3</sup>*Lawrence Livermore National Laboratory, L-414, P.O. Box 808, Livermore, CA 94551, USA*

<sup>4</sup>*Department of Physics and Astronomy, Michigan State University, East Lansing, MI 48824, USA*

<sup>5</sup>*Oak Ridge National Laboratory, P.O. Box 2008, Oak Ridge, TN 37831, USA*

We report the microscopic origins of the anomalously suppressed beta decay of  $^{14}\text{C}$  to  $^{14}\text{N}$  using the *ab initio* no-core shell model (NCSM) with the Hamiltonian from chiral effective field theory (EFT) including three-nucleon force (3NF) terms. The 3NF induces unexpectedly large cancellations within the *p*-shell between contributions to beta decay, which reduce the traditionally large contributions from the NN interactions by an order of magnitude, leading to the long lifetime of  $^{14}\text{C}$ .

PACS numbers: 21.30.Fe, 21.60.Cs, 23.40.-s

The measured lifetime of  $^{14}\text{C}$ ,  $5730 \pm 30$  years, is a valuable chronometer for many practical applications ranging from archeology to physiology. It is anomalously long compared to lifetimes of other light nuclei undergoing the same decay process, allowed Gamow-Teller (GT) beta-decay, and it poses a major challenge to theory since traditional realistic nucleon-nucleon (NN) interactions alone appear insufficient to produce the effect[1]. Since the transition operator, in leading approximation, depends on the nucleon spin and isospin but not the spatial coordinate, this decay provides a precision tool to inspect selected features of the initial and final states. To convincingly explain this strongly inhibited transition, we need a microscopic description that introduces all physically-relevant 14-nucleon configurations in the initial and final states and a realistic Hamiltonian that governs the configuration mixing.

We report the first no-core solutions of  $^{14}\text{C}$  and  $^{14}\text{N}$  using a Hamiltonian with firm ties to the underlying theory of the strong interaction, Quantum Chromodynamics (QCD), which allows us to isolate the key canceling contributions involved in this beta decay. We find that the three-nucleon force (3NF) of chiral perturbation theory (ChPT) plays a major role in producing a transition rate that is near zero, needed for the anomalous long lifetime. A chiral 3NF with coupling constants consistent with other works and within their natural range can provide the precise lifetime. This indicates that corrections to the lifetime that arise from increasing the basis space, from including additional many-body interactions and from corrections to the GT operator in ChPT [2] may be absorbed into an allowed choice of the 3NF.

Our work features two major advances over recent alternative explanations [3, 4]: (1) we treat all nucleons on the same dynamical footing with the no-core shell model (NCSM) [5], and (2) we include the 3NF of ChPT [6] as a full 3-nucleon interaction. This follows previous work detailing the structure and electroweak properties of selected  $A=10-13$  nuclei [7] with the same chiral NN + 3NF. We also establish a foundation for future work on

the GT transitions to excited  $A=14$  states [8].

ChPT provides a theoretical framework for inter-nucleon interactions based on the underlying symmetries of QCD. Beginning with pionic or the nucleon-pion system [9] one works consistently with systems of increasing nucleon number [10–12]. One makes use of the explicit and spontaneous breaking of chiral symmetry to expand the strong interaction in terms of a generic small momentum. The ChPT expansion conveniently divides the interactions into perturbative and non-perturbative elements. The latter are represented by a finite set of constants at each order of perturbation theory that are not presently obtainable from QCD, but can be fixed by experiment. These constants should be of order unity (“naturalness”). Once determined, the resulting Hamiltonian predicts all other nuclear properties. We have demonstrated that this reductive program works well for light nuclei when the 3NF is included. [7].

We adopt NN and 3NF potentials of ChPT [13, 14] and the no-core shell model (NCSM) to solve the many-body Schrödinger equation for  $A=14$  nuclei while preserving all Hamiltonian symmetries [5, 15, 16]. The non-perturbative coupling constants of the 3NF, not fixed by  $\pi - N$  or NN data, are  $c_D$  for the  $N - \pi - NN$  contact term and  $c_E$  for the  $NNN$  contact term. We previously fit  $c_D$  and  $c_E$  to  $A=3$  binding energies and selected *s*-shell and *p*-shell nuclear properties and showed the resulting interactions worked well for  $A=10-13$  nuclei [7]. Here, we present results for  $(c_D, c_E) = (-0.2, -0.205)$  and for  $(-2.0, -0.501)$ . Both sets, labeled by their  $c_D$  value below, are allowed by the naturalness criterium and fit the  $A=3$  binding energies. The former also produces a precise fit to the triton half life [17]. The latter produces the triton half life within 20% of experiment but is preferred by the  $^{14}\text{C}$  half life as we show here.

We select a basis space of harmonic oscillator (HO) single-particle states specified by the HO energy  $\hbar\Omega$  and by  $N_{max}$ , the limit on the number of HO quanta,  $\sum_i (2n_i + l_i)$ , above the minimum for that nucleus.  $n_i$  is the principal quantum number of the orbital of the  $i^{th}$

nucleon and  $l_i$  is its orbital angular momentum. Thus  $N_{max} = 0$  is the smallest basis space for each nucleus consistent with the Pauli principle. For each choice of  $N_{max}$  and  $\hbar\Omega$  we carry out a well-established finite-basis renormalization [18] of the Hamiltonian to arrive at an Hermitian effective 3-body Hamiltonian [5, 16]. All symmetries of the underlying Hamiltonian are preserved throughout. We adopt  $\hbar\Omega = 14$  MeV, which corresponds to the minimum in the binding energy obtained for  $N_{max} = 8$ . We have checked that results for  $13 \leq \hbar\Omega \leq 18$  MeV do not qualitatively alter our conclusions.

Basis space dimensions grow rapidly with  $N_{max}$  and provide a major technical challenge [19]. The many-body matrix dimension in the M-scheme basis (total magnetic projection quantum number is fixed) for  $^{14}\text{C}$  ( $^{14}\text{N}$ ) is 872,999,912 (1,090,393,922) at  $N_{max} = 8$  and the associated number of non-vanishing 3NF matrix elements on and below the diagonal  $\simeq 2.9 \times 10^{13}$  ( $\simeq 3.9 \times 10^{13}$ ).

We obtained our results on the Jaguar supercomputer at Oak Ridge National Lab [22] using up to 35,778 hex-core processors (214,668 cores) and up to 6 hours of elapsed time for each set of low-lying eigenvalues and eigenvectors. The number of non-vanishing matrix elements exceeded the total memory available and required matrix element recomputation “on-the-fly” for the iterative diagonalization process (Lanzos algorithm).

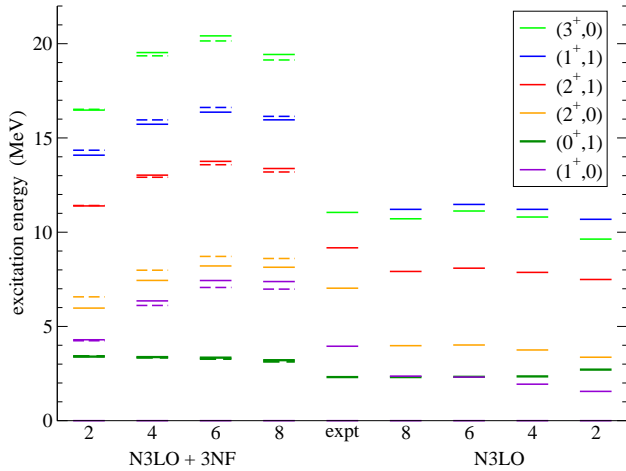


FIG. 1: (Color online) The excitation spectrum of  $^{14}\text{N}$  obtained in the NCSM using chiral interactions as a function of basis space cutoff  $N_{max}$ , the number that labels the columns.  $(J^\pi, T)$  values are in the legend. The center column displays the experimental spectrum for  $^{14}\text{N}$ . Columns to the right are obtained with the chiral NN interaction alone while those on the left are obtained with the chiral NN + 3NF using  $c_D = -0.2$  (solid lines) and  $c_D = -2.0$  (dashed lines).

Fig. 1 compares our spectra for  $^{14}\text{N}$  with experiment. The  $T = 1$  isobaric analog states serve as good proxies for the  $^{14}\text{C}$  spectra. We present the spectra as a function of the  $N_{max}$  value (column labels) for both the chiral NN

interaction alone (“N3LO” columns) and the chiral NN + 3NF (“N3LO+3NF” columns).

The trends in excitation energies with increasing  $N_{max}$  suggest reasonable convergence. We note that the level orderings are the same with and without the 3NF in the largest basis spaces ( $N_{max} = 8$ ). Overall, the spectra are more compressed with NN alone than with NN + 3NF, a pattern seen before [7, 16]. However, the 3NF appears to have over compensated for the compression in the NN spectra when compared with experiment. On the other hand the 3NF improves the binding energies. The experimental ( $^{14}\text{C}$ ,  $^{14}\text{N}$ ) binding energies are (105.28, 104.66) MeV. Without the 3NF, we obtain (97.20, 96.36) MeV. When we include the 3NF the binding energies increase to (108.43, 108.47) MeV for  $c_D = -0.2$  and (108.30, 108.41) MeV for  $c_D = -2.0$ .

We note that the binding energies for both  $^{14}\text{C}$  and  $^{14}\text{N}$  are about 8 MeV or 8% larger at  $N_{max} = 6$  than they are at  $N_{max} = 8$ . Similar calculations for lighter nuclei show that the convergence of the binding energy is not monotonic, hampering an extrapolation to the complete (infinite-dimensional) basis. On the other hand, the excitation spectra appear rather stable upon reaching  $N_{max} = 8$ . We take results in the largest available basis space as estimates of the converged results. We also show in Fig. 1 that the spectra are relatively insensitive to a significant range of values for  $(c_D, c_E)$ .

Using Fermi’s Golden rule for the transition rate, the half life  $T_{1/2}$  for  $^{14}\text{C}$  is given by

$$T_{1/2} = \frac{1}{f(Z, E_0)} \frac{2\pi^3 \hbar^7 \ln 2}{m_e^5 c^4 G_V^2} \frac{1}{g_A^2 |M_{GT}|^2}, \quad (1)$$

where  $M_{GT}$  is the reduced GT matrix element;  $f(Z, E_0)$  is the Fermi phase-space integral;  $E_0 = 156$  keV is the  $\beta$  endpoint;  $G_V = 1.136 \cdot 10^{-11}$  MeV $^{-2}$  is the weak vector coupling constant;  $g_A = 1.27$  is the axial vector coupling constant; and  $m_e$  is the electron mass.  $M_{GT}$  for the transition from the initial  $^{14}\text{C}$   $(J^\pi, T) = (0^+, 1)$  ground state  $(\Psi_i)$  to the  $^{14}\text{N}$   $(1^+, 0)$  ground state  $(\Psi_f)$  is defined by the spin-isopin operator  $\sigma(k)\tau_+(k)$  acting on all nucleons,  $k$ :

$$M_{GT} = \sum_k \langle \Psi_f | \sigma(k)\tau_+(k) | \Psi_i \rangle. \quad (2)$$

Since the initial state has total spin zero,  $M_{GT}$  is equal to the M-dependent GT matrix element  $M_{GT}^M$ ,

$$M_{GT}^M = \sum_{\alpha, \beta} \langle \alpha | \sigma \tau_+ | \beta \rangle \rho_{\alpha\beta}, \quad (3)$$

where  $\langle \alpha | \sigma \tau_+ | \beta \rangle$  is the one-body matrix element between HO single-particle states  $\alpha$  and  $\beta$ , which is non-vanishing only when both single-particle states are in the same shell, and the one-body density matrix  $\rho_{\alpha\beta} \equiv \langle \Psi_f | a_\alpha^\dagger a_\beta | \Psi_i \rangle$ .

In order to reproduce the measured half life of  $T_{1/2} \simeq 5730$  years, the GT matrix element must be anomalously small,  $|M_{GT}^M| \simeq 2 \times 10^{-3}$ , in contrast with a conventional strong GT transition in a light nucleus with  $|M_{GT}| \simeq 1$ .

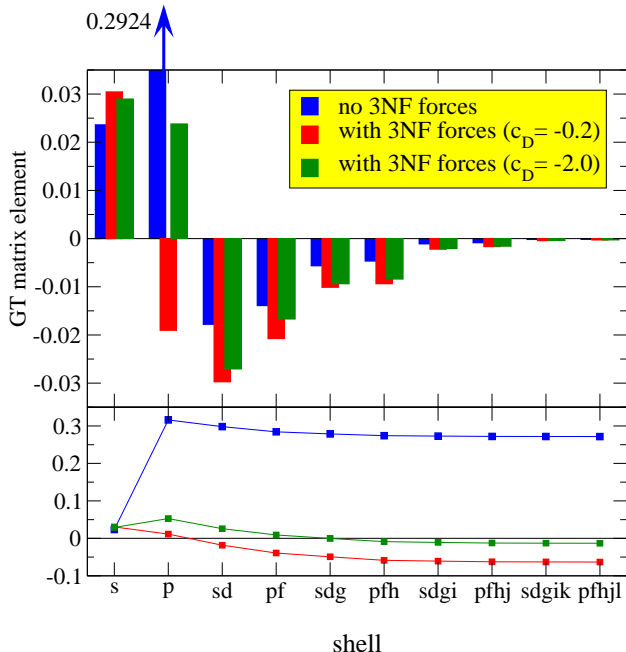


FIG. 2: (Color online) Contributions to the  $^{14}\text{C}$  beta decay matrix element as a function of the HO shell in which they are evaluated when the nuclear structure is described by the chiral interaction. Top panel displays the contributions with (two right bars of each triplet) and without (leftmost bar of each triplet) the 3NF at  $N_{max} = 8$ . All contributions are summed within the shell to yield a total for that shell. The bottom panel displays the running sum of the GT contributions over the shells included in the sum. Note the order-of-magnitude suppression of the  $p$ -shell contributions arising from the 3NF.

In Fig. 2, we present our main results for  $M_{GT}$ . We decompose  $M_{GT}$  at  $N_{max} = 8$  into the contributions arising from each HO shell for two cases with the 3NF ( $c_D = -0.2, -2.0$ ) and one without. The largest effect occurs in the  $p$ -shell where, for both values of  $c_D$ , the 3NF reduces the contributions by an order-of-magnitude from the result with the NN interaction alone. The contributions of each of the 9 additional shells is enhanced by up to a factor of 2 by the 3NF. The cumulative contributions to the GT matrix element is displayed in the lower panel of Fig. 2 where one sees clearly the net suppression to  $M_{GT}$  due to the 3NF.

Looking into the detailed changes within the  $p$ -shell, one finds that the 3NF introduces a systematic shift of strength away from 1-body density matrix terms involving transitions between the  $0p_{3/2}$  and the  $0p_{1/2}$  orbits to 1-body density matrix elements involving transitions within the  $0p_{1/2}$  orbits. The shift is about 30% of the magnitudes of these 1-body density matrix terms and

supports a recurring theme of 3NF's in  $p$ -shell nuclei - they play a significant role in the spin-sensitive properties of spin-orbit pairs. We note that our observed shifts within the  $p$ -shell due to the 3NF is similar to what Ref. [3] accomplished with a density-dependent effective NN interaction obtained by modeling leading contributions from the chiral 3NF. However, our net contributions from other shells, which are absent in Ref. [3], overwhelm the net  $p$ -shell contribution as seen in Fig. 2. That is, while the  $s$ -shell and  $sd$ -shell contributions nearly cancel, all the shells above the  $sd$ -shell contribute about a factor 2 greater than the now-suppressed  $p$ -shell contribution.

To further understand the role of the 3NF, we can examine the contributions to  $M_{GT}$  in the LS-scheme where the single-particle quantum numbers now involve the orbital angular momentum projection  $m_l$  and spin projection  $m_s$  replacing the total angular momentum projection  $m_j$ . This is a convenient representation for this transition since  $m_l$  and  $m_s$  must be the same for incoming and outgoing single-particle states. For the  $p$ -shell contributions, the resulting decomposition to LS-scheme yields results shown in Table I. Note that there is nearly perfect cancellation between the  $m_l = 0$  and  $m_l = \pm 1$  terms once the 3NF is included.

Given the overall effects on  $M_{GT}$  by inclusion of the 3NF as seen through Fig. 2 and in Table I, one may fine tune  $c_D$  to reproduce the value  $2 \times 10^{-3}$  consistent with the  $^{14}\text{C}$  lifetime. This is analogous to the fine tuning of  $c_D$  in Ref. [17] to fit the  $^3\text{H}$  lifetime. Our estimate that the desired suppression of  $M_{GT}$  occurs with  $c_D \simeq -2.0$  illustrates this point. Note that the spectra of  $^{14}\text{C}$  and  $^{14}\text{N}$  are rather insensitive to this range of  $c_D$  values. We show the resulting  $M_{GT}$  in the final row of Table I.

$(m_l, m_s)$	NN only	NN + 3NF $c_D = -0.2$	NN + 3NF $c_D = -2.0$
$(1, +\frac{1}{2})$	0.015	0.009	0.009
$(1, -\frac{1}{2})$	-0.176	-0.296	-0.280
$(0, +\frac{1}{2})$	0.307	0.277	0.283
$(0, -\frac{1}{2})$	0.307	0.277	0.283
$(-1, +\frac{1}{2})$	-0.176	-0.296	-0.280
$(-1, -\frac{1}{2})$	0.015	0.009	0.009
Subtotal	0.292	-0.019	0.024
Total Sum	0.275	-0.063	-0.013

TABLE I: Decomposition of  $p$ -shell contributions to  $M_{GT}$  in the LS-scheme for the beta decay of  $^{14}\text{C}$  without and with 3NF. The 3NF is included at two values of  $c_D$  where  $c_D \simeq -0.2$  is preferred by the  $^3\text{H}$  lifetime and  $c_D \simeq -2.0$  is preferred by the  $^{14}\text{C}$  lifetime. The calculations are performed in the  $N_{max} = 8$  basis space with  $\hbar\Omega = 14$  MeV.

Next, we studied the sensitivity at  $(c_D, c_E) = (-2.0, -0.501)$  and at  $N_{max} = 6$  by successively setting each to zero while keeping the other fixed. The larger effect on  $M_{GT}$  appears with  $c_D = 0$ . However, the resulting shifts in the magnitude of  $M_{GT}$  are approximately

proportional to the magnitude of the changes in  $c_D$  and  $c_E$  which implies  $M_{GT}$  has about the same sensitivity to each. This sensitivity differs from that of Ref. [3] where the  $c_E$  term was found to play a leading role in  $M_{GT}$ .

Since both appear natural, we conclude that the different values of  $c_D$  from the beta decays of  $^3\text{H}$  and  $^{14}\text{C}$  accommodate the sum of higher-order effects: meson-exchange currents, additional ChPT interaction terms, and contributions from larger basis spaces. Additional 3NF terms, e.g. those arising at the  $\text{N}^3\text{LO}$  level of ChPT that do not impact the  $^3\text{H}$  lifetime [20], and/or four nucleon interaction terms may impact  $^{14}\text{C}$  and  $^{14}\text{N}$ .

In order to further test the *ab initio* wavefunctions and the effects of the 3NF, we present in Table II the contributions to selected electromagnetic properties of  $^{14}\text{N}$ . We see that the 3NF has substantial influence on the magnetic-dipole transition in  $^{14}\text{N}$  from the ground state (GS) to the  $(0^+, 1)$  analog state of the  $^{14}\text{C}$  GS though the mechanism for this suppression is quite different from the GT transition. In this M1 transition, we find significant cancellation between the nucleon spin and proton angular momentum contributions. Without the 3NF, spin and angular momentum contributions add constructively. Electric properties such as the charge radius ( $RMS$ ) and the electric quadrupole moment ( $Q$ ) are reduced when we include 3NF due, in part, to the increased binding. Also, the GS magnetic moment ( $\mu$ ) is modified by 10% when we include 3NF. We expect  $RMS$  and  $Q$  to increase with basis space size while the GS energy,  $\mu$  and the B(M1) will be less effected. The role of the 3NF on the electroweak properties of these nuclei is indeed multi-faceted.

Observable	Experiment [21]	NN only	NN + 3NF $c_D = -0.2$	NN + 3NF $c_D = -2.0$
$RMS$	2.42(1)	2.28	2.25	2.24
$Q$	1.93(8)	1.87	1.03	1.19
$\mu$	0.404	0.379	0.347	0.347
B(M1)	0.047(2)	1.002	0.037	0.098

TABLE II: Properties of  $^{14}\text{N}$  without and with 3NF in the  $N_{max} = 8$  basis space with  $\hbar\Omega = 14$  MeV. The magnetic moments, which tend to converge rapidly, are obtained at  $N_{max} = 6$ . The point proton root-mean-square radius ( $RMS$ ) is quoted in fm. We corrected the measured charge radius (2.56(1) fm) for the finite proton charge contribution. The magnetic moment  $\mu$  is in nuclear magnetons  $e\hbar/2mc$ ; and the quadrupole moment is in  $e^2 fm^4$  (all for the GS). The B(M1) is the transition from the GS to the  $(0^+, 1)$  state (the isobaric analog of the  $^{14}\text{C}$  GS).

In conclusion, the chiral 3NF in *ab initio* nuclear physics produces a large amount of cancellation in the matrix element  $M_{GT}$  governing the beta decay of  $^{14}\text{C}$ . This cancellation signals a major signature of 3NF effects in the spin-isopin content of the  $0p$  orbitals in  $^{14}\text{C}$  and  $^{14}\text{N}$ . The 3NF, particularly through its longest range two-pion exchange component, modifies the  $0p$  spin-orbit pairs in the ground states of these nuclei to produce the

suppression of  $M_{GT}$  consistent with the anomalous long lifetime of  $^{14}\text{C}$ .

This work was supported in part by US DOE Grants DE-FC02-09ER41582 (UNEDF SciDAC Collaboration), DE-FG02-87ER40371, and by US DOE Contract No. DE-AC52-07NA27344 and No. DE-AC05-00OR22725. Computational resources were provided by Livermore Computing at LLNL and by a “Petascale Early Science Award” and an INCITE Award on the Jaguar supercomputer at the Oak Ridge Leadership Computing Facility at ORNL [22] which is supported by the DOE Office of Science under Contract DE-AC05-00OR22725.

- 
- [1] S. Aroua, *et al.*, Nucl. Phys. A **720** 71(2003).
  - [2] S. Vaintraub, N. Barnea and D. Gazit, Phys. Rev. C **79**, 065501(2009) [arXiv:0903.1048 [nucl-th]].
  - [3] J. W. Holt, N. Kaiser and W. Weise, Phys. Rev. C **81**, 024002(2010).
  - [4] J. W. Holt, *et al.*, Phys. Rev. Lett. **100** 062501(2008); and refs. therein.
  - [5] P. Navrátil, J. P. Vary and B. R. Barrett, Phys. Rev. Lett. **84**, 5728(2000); Phys. Rev. C **62**, 054311(2000).
  - [6] S. Weinberg, Physica **96A**, 327(1979); Phys. Lett. B **251**, 288(1990); Nucl. Phys. B **363**, 3(1991).
  - [7] P. Navrátil, *et al.*, Phys. Rev. Lett. **99** 042501(2007).
  - [8] A. Negret *et al.*, Phys. Rev. Lett. **97** 062502(2006).
  - [9] V. Bernard *et al.*, Int. J. Mod. Phys. E **4**, 193(1995).
  - [10] C. Ordonez, L. Ray, and U. van Kolck, Phys. Rev. Lett. **72**, 1982(1994); Phys. Rev. C **53**, 2086(1996).
  - [11] U. van Kolck, Prog. Part. Nucl. Phys. **43**, 337(1999).
  - [12] P. F. Bedaque and U. van Kolck, Annu. Rev. Nucl. Part. Sci. **52**, 339(2002); E. Epelbaum, Progr. Part. Nucl. Phys. **57**, 654 (2006).
  - [13] E. Epelbaum, W. Glöckle, and Ulf-G. Meissner, Nucl. Phys. A **637**, 107(1998); A **671**, 295(2000).
  - [14] D. R. Entem and R. Machleidt, Phys. Rev. C **68** 041001(R)(2003).
  - [15] P. Navrátil, Few Body Systems **41**, 117(2007).
  - [16] P. Navrátil and W. E. Ormand, Phys. Rev. Lett. **88**, 152502(2002).
  - [17] D. Gazit, S. Quaglioni and P. Navrátil, Phys. Rev. Lett. **103**, 102502(2009) [arXiv:0812.4444 [nucl-th]].
  - [18] J. Da Providencia and C. M. Shakin, Ann. of Phys. **30**, 95 (1964); K. Suzuki and S.Y. Lee, Prog. Theor. Phys. **64**, 2091 (1980); K. Suzuki, Prog. Theor. Phys. **68**, 246 (1982); K. Suzuki, Prog. Theor. Phys. **68**, 1999 (1982); K. Suzuki and R. Okamoto, Prog. Theor. Phys. **92**, 1045 (1994).
  - [19] P. Sternberg, *et al.*, In Proc. 2008 ACM/IEEE Conf. on Supercomputing (Austin, Texas, November 15 - 21, 2008); J. P. Vary, *et al.*, Jnl of Phys: Conf. Series **180**, 12083 (2009); P. Maris, *et al.*, ICCS 2010, Procedia Computer Science **1**, 97(2010).
  - [20] A. Gardestig and D. R. Phillips, Phys. Rev. Lett. **96**, 232301 (2006) [arXiv:nucl-th/0603045].
  - [21] F. Ajzenberg-Selove, Nucl. Phys. A **523** 1(1991); TUNL Nuclear Data Evaluation Group (www.tunl.duke.edu).
  - [22] Information on Jaguar can be found at www.ncs.gov